

*Short Communication*

## **Effect of Anodic Films on Corrosion Resistance and Fatigue Crack Initiator of 2060-T8 Al-Li Alloy**

Y.Z. Shen, H.G. Li, H.J. Tao, J. Ling, T. Wang and J. Tao \*

College of Material Science and Technology, Nanjing University of Aeronautics and Astronautics,  
Nanjing 210016, P. R. China

\*E-mail: [taojie@nuaa.edu.cn](mailto:taojie@nuaa.edu.cn)

*Received:* 3 October 2014 / *Accepted:* 31 October 2014 / *Published:* 2 December 2014

---

Two kinds of anodic films (i.e., CAA films and BSAA films) on surfaces of 2060 Al-Li alloy were successfully prepared by anodizing. The presenting work mainly focused on the contrastive investigation about the effect of the two kinds of anodic films on corrosion resistance and fatigue crack initiator. The morphologies of the samples were characterized by scanning electron microscopy (SEM), and the bonding strength between films and substrate was tested by WS-2005 automatic scratch tester. It was found experimentally that the two kinds of anodic films had nearly the same corrosion resistance and bonding strength between the films and substrates. However, the CAA films had a greater influence on the fatigue crack initiator of 2060-T8 Al-Li alloy comparing to BSAA films.

---

**Keywords:** Aluminium, Anodizing, Anti-corrosion, Fatigue

### **1. INTRODUCTION**

Al-Li alloy has become a promising light-weight material for aerospace application in the future owing to its excellent properties, such as high specific strength, high specific stiffness, low density, and fatigue resistance [1-3]. However, relatively poor corrosion resistance has restricted its application to a certain extent in many harsh environments. Although a layer of nature oxide films can be formed on the surface of Al-Li alloy, they cannot provide sufficient corrosion resistance for the conventional corrosion protection [4]. Anodizing of aluminum alloy is a widely researched and accepted method to manufacture alumina films on the surface for enhancing the corrosion resistance [5-6].

Currently, chromic acid anodization (CAA) is widely employed for corrosion prevention owing to the existence of the hexavalent chromium compounds (efficient corrosion inhibitors) in the anodic films [7]. As a consequence, the corrosion resistance of the Al-Li alloy is greatly enhanced. However,

CAA technique has a fatal weakness that chromium VI is a highly toxic pollutant to the natural environment. Since 2006, EU environmental legislations have banned the use of the hexavalent chromium compounds in industry. Thus, many researchers gradually pay greater attention on non-Cr (VI) conversion process to prepare oxide films. As early as in 1990, the engineers in Boeing Company developed and qualified the Boric Sulfuric Acid Anodization (BSAA) technique as a chromic acid anodization replacement [8]. It is regarded as an environment-friendly anodizing technique and also provides a high corrosion resistance. In the last two decades, researchers perform a large number of experiments to optimize the BASS films on the various series of Al alloy [9]. Therefore, BASS technique is gradually applied in the aviation industry owing to the characteristic of non-pollution to environment.

However, as for anodizing behavior of Al and its alloy, it has an intrinsically adverse effect on fatigue life, which is attributed to the brittle and porous oxide layer and the residual stress induced during the anodizing process [10]. Under the tensile cyclic stress, anodic film cracks easily and fatigue crack initiator occurs because of the fragility of oxide layer, which results in a reduction in fatigue life [11]. To successfully apply an environment-friendly anodizing technique on the lightweight Al-Li alloy, an equal or greater resistance of the anodic films to fatigue and corrosion needs to be evaluated.

In this work, we evaluated the corrosion resistances and fatigue resistances of the anodized 2060-T8 Al-Li alloy with CAA process and BSAA process at the 70% stress level, respectively. Meanwhile, observing the surface morphologies and fractographies of samples, we analyzed the effect of anodic films on inducing fatigue crack initiator.

## 2. EXPERIMENTAL PROCEDURE

### 2.1 Specimen preparation

**Table 1.** Chemical composition of 2060 Al-Li alloy (wt %)

Si	Fe	Cu	Mn	Mg	Zn	Ag	Li	Zr	Al
0.01	0.02	3.7	0.29	0.7	0.34	0.34	0.8	0.11	Bal.

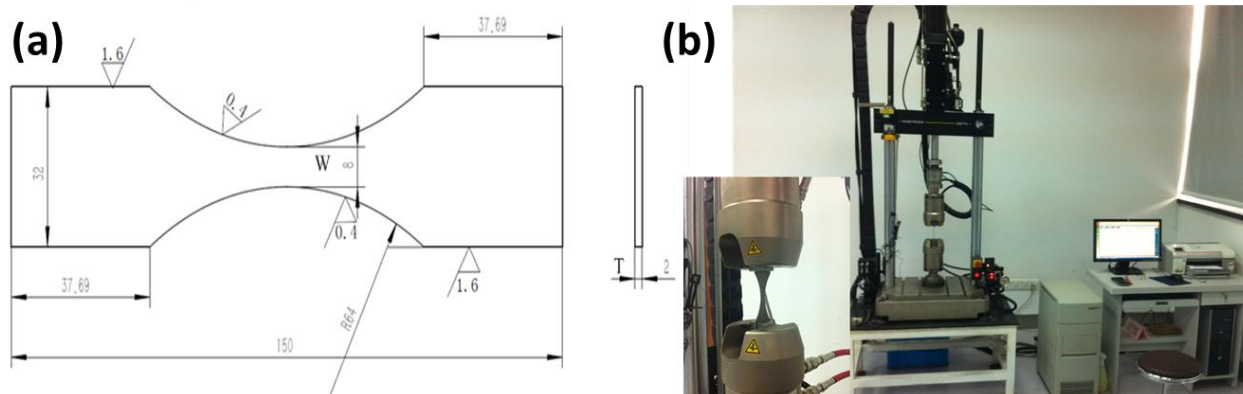


**Figure 1.** *a* The size of fatigue test specimens (dimensions in mm); *b* INSTRON 8874 test system

2060 Al-Li T8 alloy was provided by commercial aircraft corporation of china, Ltd. The average chemical composition of the Al-Li alloy is given in Table 1. According to ASTM E466, the specimens were manufactured with an appropriate size, as shown in Fig. 1a. The roughness ( $R_a$ ) of test section was about 0.4  $\mu\text{m}$ , and the ratio of specimen test section width (W) to thickness (T) was 4. All the specimens' axial directions were parallel to the rolling direction of Al-Li T8 alloy plate.

## 2.2 Anodic oxidation process

Prior to anodizing, alkaline cleaning for the specimens was performed in the solution of 15 g L<sup>-1</sup> NaOH, 12 g L<sup>-1</sup> Na<sub>2</sub>CO<sub>3</sub> and 10 g L<sup>-1</sup> Na<sub>3</sub>PO<sub>4</sub> at 65-70 °C for 2-3 min. Subsequently, the specimens were immersed in 25% HNO<sub>3</sub> aqueous solution at room temperature for 15-20 s. After each step, the specimens were rinsed in distilled water and dried in the air.

CAA was carried out in chromic acid solution (45 g L<sup>-1</sup>) with a constant voltage of 20 V at 35 °C for 35 min. And according to BAC 5632, BSAA was also performed in the solution containing 40 g L<sup>-1</sup> H<sub>2</sub>SO<sub>4</sub> and 8 g L<sup>-1</sup> H<sub>3</sub>BO<sub>3</sub> with a constant voltage of 15 V at 25 °C for 20 min. The both anodizing experiments were operated with a programmable D.C power supply (WYK-1502, Yangzhou Aikesai Electronic Co., Ltd., China). After anodizing, the specimens were rinsed in distilled water. Finally, it was necessary to perform the sealing treatment in boiling distilled water (> 95 °C) for 20 min to enhance corrosion resistance.

## 2.3 Film characterization

The surface and section morphologies were observed by scanning electron microscope (SEM; Quanta200, FEI Company, US). The electrochemical corrosion behaviors of the anodic films were characterized by potentiodynamic polarization, which were conducted with a scan rate of 0.01 V/s by a CHI660d electrochemical analyzer (Shanghai, China) in 3.5% NaCl solution at room temperature. Before testing, we tested one sample with a lower scan rate (0.001 V/s). It was found that the result was nearly same as that with the scan rate of 0.01 V/s. Thus, in this test, the scan rate of 0.01 V/s was appropriate, and the test results with this rate were more repeatable comparing with a lower scan rate. Furthermore, A Pt plate and a saturated calomel electrode (SCE) were used as the counter electrode and the reference electrode, respectively. Before testing, the specimens were immersed in NaCl solution for about 0.5 h in order to stabilize the open circuit potential. The bonding strength between films and substrate was tested by WS-2005 automatic scratch tester (Lanzhou, China) with a radius of 0.2 mm diamond indenter at the speed of 5 mm min<sup>-1</sup> to move ahead and with a loading rate (50 N min<sup>-1</sup>).

## 2.4 Fatigue testing

The axial fatigue tests were performed at 15 Hz in ambient conditions at stress ratio R=0.1 using a 25 kN servo-hydraulic INSTRON machine (Seeing Fig. 1b). The maximum cyclic stress ( $\sigma_{\text{max}}$ )

was set at a value of 70 % ultimate strength ( $\sigma_b$ ) for expecting to result in a fatigue life between  $10^4$  to  $10^6$  cycles. And the fatigue life of each specimen was calculated with five measured values. Therefore, we tested its ultimate strength at a loading rate of  $2 \text{ mm min}^{-1}$ , and the result showed that it was 490.06 MPa.

### 3. RESULTS AND DISCUSSION

#### 3.1 Surface and cross-section morphologies

The surface and cross-section morphologies of anodic films before any fatigue testing are revealed in Fig. 2. It can be found that many pores appear on the surface, owing to the breakdown caused by applied voltage and the corrosion effect of electrolyte to anodic films. Furthermore, the pore depth of anodic films prepared by CAA process is greater than that of anodic films fabricated by BSAA process. But observing the cross-section morphologies, the two kinds of anodic films are crackless and compact. And the anodic films tightly adhere to the substrates from Fig. 2c and d owing to the in-situ growth behavior of anodizing. Meanwhile, we find that some main elements from electrolyte, such as Cr and S, have spread into the films and O element in the films has also diffused into the substrate according to the element distribution curve in Fig. 2c and d.

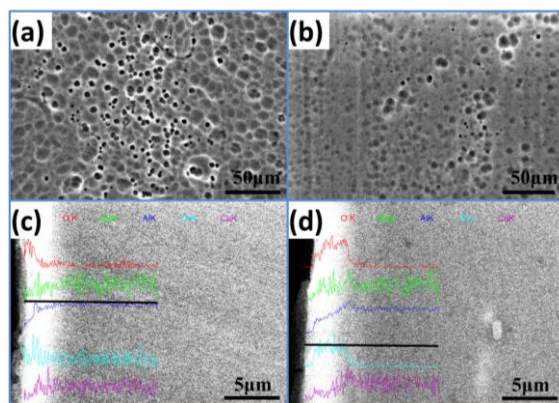


**Figure 2.** The surface and cross-section morphologies of anodic films, (a) and (c) CAA; (b) and (d) BSAA

#### 3.2 The bonding force between anodic films and substrate

The bonding force between anodic films and substrate is also revealed via the scratch adhesion test curves, as shown in Fig. 3. The acoustic emission signal received by the test means that the films begin to desquamate or the indenter meets one deeper pit. Herein, when a large number of acoustic emission signals are received, the critical load is measured as the bonding force between the films and substrate. The results shown in Fig. 3 indicate that the bonding forces of two kinds of anodic films with substrate are both 70 N.

However, when the load is about 45 N, some acoustic emission signals are also captured by the machine. We believe that the indenter meets a deep pit at this moment, which results in some acoustic emission signals being received. Observing the surface morphologies, there are many pits appearing on the surface of anodic films owing to the corrosion effect of electrolyte to anodic films. Thus, the conclusion can be drawn that the bonding force between anodic films and substrate is about 70 N, regardless of what kind of anodic oxidation process. And S. Hogmark concluded that, referring to bonding force between the films and substrate, a critical load of 30 N was sufficient to meet the application requirement of practical wear and sliding friction [12]. Hence, the bonding force of as-prepared anodic films is both far more than 30 N, indicating that the films are well bonded.

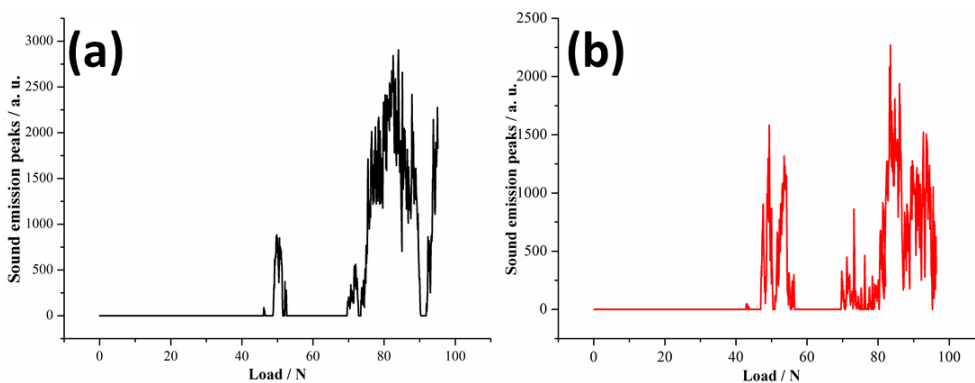


**Figure 3.** Scratch adhesion test curves of anodic films, (a) CAA anodic films; (b) BSAA anodic films

### 3.3 Corrosion resistance

As an important performance, corrosion resistance of anodic films should be evaluated. The polarization curves of anodic films, prepared with CAA process and BSAA process, in 3.5% NaCl solution are shown in Fig. 4. And the corrosion potential and corrosion current are calculated and listed in Table 2.

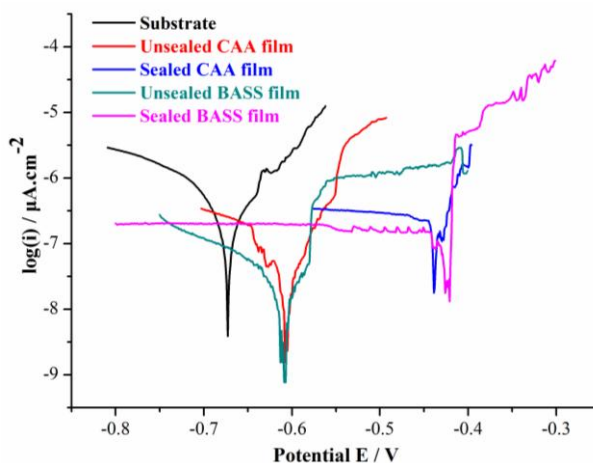


**Figure 4.** Polarization curves of anodic films in 3.5% NaCl solution

Comparing with substrate, the sealed anodic films both show excellent corrosion resistance with a higher corrosion potential and a less corrosion current in a 3.5% NaCl solution. In this study, the corrosion potential of the sealed BASS films can reach about -0.42 V, and its corrosion current also decreases to  $7.277 \times 10^{-8}$ . Remarkably, its corrosion resistance is even greater than that of CAA films owing to the uniform and smooth microscopic surface (Seeing Fig. 2a and b). Comparing to the other samples, the sample (Sealed BASS film) has the highest values of anodic and cathode slopes (6.394 and 21.368), seeing Table 2. This may be explained by the fact that anodic and cathodic reactions are difficult to occur owing to the relatively uniform and compact anodic films. In the chromic acid electrolyte, the hexavalent chromium compounds can be synthesized and diffuse into anodic films. But chromic acid has the non-ignorable erosion effect on the anodic films, which results in some deeper pits emerging on the surface. However, in the mixed solution of boric acid and sulfuric acid, the surface of anodic films is more smooth and flat owing to the adding the extremely weak boric acid. Thus, the BSAA films show a little greater corrosion resistance than CAA films, which is caused by the smooth and flat surface.

**Table 2.** The fitting data of the polarization curve

	Substrate	Unsealed CAA film	Sealed CAA film	Unsealed BASS film	Sealed BASS film
Corrosion Potential / V	-0.673	-0.607	-0.438	-0.608	-0.421
Corrosion Current / $\mu\text{A}\cdot\text{cm}^{-2}$	$3.284 \times 10^{-7}$	$6.776 \times 10^{-8}$	$4.307 \times 10^{-7}$	$2.536 \times 10^{-8}$	$7.277 \times 10^{-8}$
$\beta_c$ (1/V)	5.233	4.876	6.332	4.732	6.394
$\beta_a$ (1/V)	18.214	14.327	20.981	13.480	21.368

### 3.4 Fatigue performance and fractography

The aim of anodizing of aluminum alloy is to improve the corrosion resistance for meeting some practical applications, but which also results in producing fatigue crack initiator. The fatigue life of the anodized 2060-T8 Al-Li alloy with CAA process and BSAA process at the 70% stress level of ultimate strength is shown in Fig. 5. If the fatigue life of substrate is considered as 100%, the fatigue life of anodized 2060-T8 Al-Li alloy with CAA process is only 87.5%, but the BSAA films do not have such a great influence on the fatigue life with the value of 97.2%.

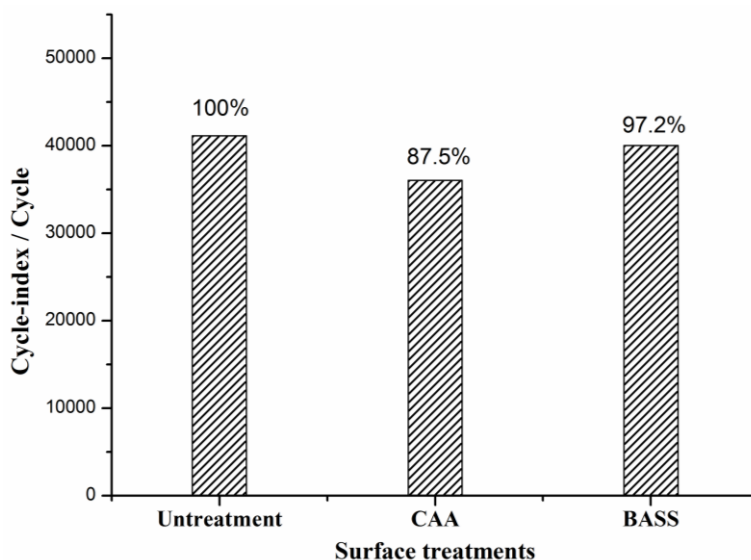


**Figure 5.** The fatigue life of the anodized 2060-T8 Al-Li alloy

In order to understand the fatigue damage behavior under anodized conditions, the fractographic morphologies of the anodized fatigue test specimen with CAA process are obtained in Fig. 6. The typical fractographs of fatigue test specimen, including fatigue crack initiator (Fig. 6b), fatigue crack propagation (Fig. 6c) and dimple feature of instantaneous fracture (Fig. 6d), are revealed clearly, Which also has a strong evidence that the fatigue crack initiator is at the pittings of the anodic films.

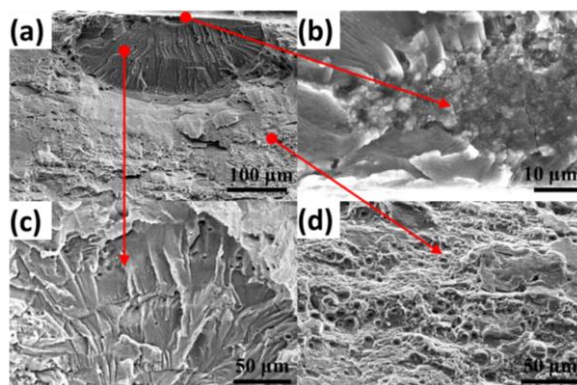


**Figure 6.** Fractographs of the anodized fatigue test specimen with CAA process, (a) X 200; (b) X 2000; (c) X 500; (d) X 500

As a matter of fact, it has been confirmed that the fatigue resistance of aluminum alloy depends on the fatigue crack initiator, suggesting that reducing the number of fatigue crack initiators is of great significance to decrease the effect of anodic films on the fatigue performance [13]. As we all know, when the hard anodic films are produced under the electrochemical reaction, the residual stress will be produced due to the difference of the intrinsic property of the substrate and oxidation films.

Furthermore, the residual stress mainly concentrates in the pores of the anodic films, resulting in producing the fatigue crack initiator. According to the analysis of surface morphologies of the anodic films, more pores appear on the surface of CAA films than that of BSAA films. In addition, the pore depth of anodic films prepared by CAA process is greater than that of anodic films fabricated by BSAA process. Thus, the BSAA films have trifling influence on the fatigue life of 2060-T8 Al-Li alloy (the value of fatigue life is 97.2%). For other aluminium alloy, some similar results have been also reported. Michel Chaussumier's research group investigated the effect of sealed anodic film on fatigue performance of 2214-T6 aluminum alloy, and found that the decrease in fatigue life was mainly attributed to the generation of fatigue crack initiator [14]. Thus, BSAA films, relatively flat surface comparing to the CAA films, can induce less fatigue initiator.

#### 4. CONCLUSIONS

In summary, by the contrastive investigation of the two kinds of anodic films, BSAA films possessed the almost same corrosion resistance as CAA films. The bonding force between films and substrate was both up to 70 N owing to the in-site growth behavior of anodic oxidation. However, the BSAA films had a weaker influence on the fatigue crack initiator of 2060-T8 Al-Li alloy than CAA films. Thus, environment-friendly BSAA technique could replace the CAA technique to prepare anodic films for industrial applications.

#### ACKNOWLEDGEMENTS

The authors gratefully acknowledge the financial support of the National Science Foundation of China (No. 51202112), the Fund of National Engineering and Research Center for Commercial Aircraft Manufacturing (No: SAMC13-JS-15-032), the Jiangsu Innovation Program for Graduate Education (KYLX\_0261), the Fundamental Research Funds for the Central Universities (NZ2013307), and the Foundation of Graduate Innovation Center in NUAA (Grant No. kfjj20130220).

#### References

1. S.F. Zhang, W.D. Zeng, W.H. Yang, C.L. Shi and H.J. Wang, *Mater. Design*, 63 (2014) 368-374
2. R.K. Gupta, N. Nayan, G. Nagasireesha and S.C. Sharma, *Mat. Sci. Eng. A.*, 420 (2006) 228-234
3. M.E. Krug, Z.G. Mao, D.N. Seidman and D.C. Dunand, *Acta. Mater.*, 79 (2014) 382-395
4. G. Ruhi, O.P. Modi, A.S. K. Sinha and I.B. Singh, *Corros. Sci.*, 50 (2008) 639-649
5. M. Saeedikhani, M. Javidi and A. Yazdani, *T. Nonferr Metal Soc.*, 23 (2013) 2551-2559
6. M. Shahzad, M. Chaussumier, R. Chieragatti, C. Mabru and F. Rezai-Aria, *Mater. Design*, 32 (2011) 3328-3335
7. M. Chaussumier, C. Mabru, R. Chieragatti and M. Shahzad, *Procedia Eng.*, 66 (2013) 300-312
8. J.S. Zhang, X.H. Zhao, Y. Zuo and J.P. Xiong, *Surf. Coat. Tech.*, 202 (2008) 3149-3156
9. S.J. Ma, P. Luo, H.H. Zhou, C.P. Fu and Y.F. Kuang, *T. Nonferr. Metal. Soc.*, 18 (2008) 825-830
10. B.H. Nie, Z. Zhang, Z.H. Zhao and Q.P. Zhong, *Mater. Design*, 50 (2013) 1005-1010
11. M. Shahzad, M. Chaussumier, R. Chieragatti, C. Mabru and F. Rezai-Aria, *Procedia Eng.*, 2 (2010) 1015-1024
12. S. Hogmark, S. Jacobson and M. Larsson, *Wear*, 246 (2000) 20-33

13. J.A.M. Camargo, H.J. Cornelis, V.M.O.H. Cioffi and M.Y.P. Costa, *Surf. Coat. Tech.*, 201 (2007) 9448-9455
14. M. Shahzad, M. Chaussumier, R. Chieragatti, C. Mabru and F. Rezai-Aria, *Surf. Coat. Tech.*, 206 (2012) 2733-2739.

© 2015 The Authors. Published by ESG ([www.electrochemsci.org](http://www.electrochemsci.org)). This article is an open access article distributed under the terms and conditions of the Creative Commons Attribution license (<http://creativecommons.org/licenses/by/4.0/>).